Inorg. Chem. **2006**, *45*, 3456–3466

Cu(I) Dinuclear Complexes with Tripodal Ligands vs Monodentate Donors: Triphenylphosphine, Thiourea, and Pyridine. A ^{1}H NMR Titration Study

Marcello Gennari, Maurizio Lanfranchi, Luciano Marchiò,* Maria Angela Pellinghelli, Matteo Tegoni, and Roberto Cammi

Dipartimento di Chimica Generale ed Inorganica, Chimica Analitica, Chimica Fisica, Università degli Studi di Parma, Parco Area delle Scienze 17a, I 43100 Parma, Italy

Received December 13, 2005

Complexes [$PPh_3Cu(Tr^{Mes,Me}$)] (**1**), [$PPh_3Cu(Tr^{Me,o-Py}$)] (**2**), and [$PPh_3Cu(Br^{Mes}pz^{o-Py}$)] (**3**) ($Tr^{Mes,Me}$ = hydrotris[1,4-dihydro-3-methyl-4-mesityl-5-thioxo-1,2,4-triazolyl]borate; $Tr^{Me,o-Py}$ = hydrotris[1,4-dihydro-4-methyl-3-(2-pyridyl)-5-thioxo-1,2,4-triazolyl]borate; $Br^{Mes}pz^{o-Py}$ = hydro[bis(thioxotriazolyl)-3-(2-pyridyl)pyrazolyl]borate; PPh_3 = triphenylphosphine) were synthesized by the reaction of dinuclear complexes [$Cu(Tr^{Mes,Me})]_2$, [$Cu(Tr^{Me,o-Py})]_2$, [$Cu(Br^{Mes}pz^{o-Py})]_2$, and PPh_3. **1**–**3** were characterized by ^{1}H, ^{13}C, and ^{31}P NMR spectroscopy and ESI-mass spectrometry. Crystal structure analyses were performed for **1** and **2**. Both complexes crystallize in the triclinic $P\bar{1}$ space group with the metal in a slightly distorted tetrahedral geometry (S_3P coordination) bound by a κ^3-S_3 ligand and a PPh_3 molecule. The solution molecular structures were investigated by means of variable-temperature (210–310 K, $CDCl_3$, **1**–**2**; 200–310 K, CD_2Cl_2, **3**) and NOESY NMR spectroscopy. The solution structures of **1**–**2** are in accordance with the X-ray structures, and the complexes do not exhibit fluxional behavior. On the other hand, **3** is subject to an equilibrium between two species with a coalescing temperature of ~260 K. DFT geometry optimizations suggest that the major species of **3** consists of the $Br^{Mes}pz^{o-Py}$ ligand bound to Cu(I) in the κ^3-S_2H fashion with two C=S groups and a [Cu···H–B] interaction. A PPh_3 completes the copper coordination (S_2HP coordination). The complex [TuCu($Tr^{Mes,Me}$)] (**4**) (Tu = thiourea) was crystallized using an excess of Tu with respect to [$Cu(Tr^{Me,2-Py})]_2$ (approximately a 6:1 ratio). The metal adopts a distorted tetrahedral geometry with an overall S_3H coordination determined by the bound κ^3-S_2H ligand (two C=S groups and a [B–H···Cu] interaction) and by a Tu. The reactivity of dinuclear complexes [$Cu(Tr^{Mes,Me})]_2$, [$Cu(Tr^{Me,o-Py})]_2$, and [$Cu(Br^{Mes}pz^{o-Py})]_2$ with monodentate ligands was investigated by means of NMR titrations with PPh_3, Tu. and pyridine (Py), and formation constants for the adducts [DCu(L)] (D = monodentate donor, L = tripodal ligand) were determined.

1. Introduction

In a previous study, we investigated copper(I) complexes with tripodal S_3 and S_2N donor ligands as models for type I centers present in electron-transfer metalloproteins. For the synthesis of these compounds, a 1:1 metal:ligand ratio was always employed, with the aim of obtaining mononuclear species with a fixed geometry of donor atom sets. Despite that, dinuclear complexes were always obtained and, most importantly, they exhibited fluxional behavior in solution, making them poor candidates for copper protein type I center models.[1] This is not a surprising feature of copper(I) compounds and can be rationalized in terms of the lability and various energetically accessible geometries of copper(I).[2] In the present work, to further investigate the properties of [$Cu(Tr^{Mes,Me})]_2$, [$Cu(Tr^{Me,o-Py})]_2$, and [$Cu(Br^{Mes}pz^{o-Py})]_2$ complexes, we followed their reactions with monodentate ligands such as PPh_3, Tu, and Py by means of NMR titrations.[3] These ligands were chosen to provide a varied donor set (P, S, and N) and allowed us to evaluate the

* To whom correspondence should be addressed. E-mail: marchio@unipr.it.

(1) Cammi, R.; Gennari, M.; Giannetto, M.; Lanfranchi, M.; Marchio, L.; Mori, G.; Paiola, C.; Pellinghelli, M. A. *Inorg. Chem.* **2005**, *44*, 4333−4345.

(2) (a) Smith, D. R. *Coord. Chem. Rev.* **1998**, *172*, 457−573. (b) Melnik, M.; Macaskova, L.; Holloway, C. E. *Coord. Chem.. Rev.* **1993**, *126*, 71−92.

10.1021/ic052129l CCC: $33.50
Published on Web 03/21/2006

stability of the dinuclear complexes against σ-donors. Furthermore, this also provided the formation constant of the ternary adduct [DCu(L)] (D = monodentate donor; L = tripodal ligand), which is important for the interpretation of possible equilibria occurring in solution. The molecular structures of the ternary complexes [DCu(L)] were investigated by means of X-ray crystallography, 2D NMR spectroscopy, and in some cases by DFT calculations. The X-ray crystal structures of [$PPh_3Cu(Tr^{Mes,Me}$)] and [$PPh_3Cu(Tr^{Me,o-Py}$)] are presented and reveal the almost-regular tetrahedral copper coordination with ligands κ^3-S_3 coordinated as reported for copper(I) complexes with κ^3-S_3 thioether ligands[4] and with hydrotris(3-methyl-1-imidazolyl-2-thione)borate (Tm).[5] In the absence of the [$PPh_3Cu(Br^{Mes}pz^{o-Py}$)] X-ray structure, we employed DFT calculations to propose a molecular structure and explain the fluxional behavior of the complex according to variable temperature (VT) NMR experiments performed in $CDCl_3$. Interestingly, this equilibrium does not imply a PPh_3 dissociation, as was reported for Cu(I) complexes of tridentate κ^3-S_3 ligands and PPh_3,[4e,5] but is associated with the conformational rearrangement of $Br^{Mes}pz^{o-Py}$. To favor the crystallization of the complexes with Tu, we employed a large excess of Tu, and only [$((NH_2)_2CS)Cu(Tr^{Mes,Me})$] was crystallographically characterized. In this complex, the ligand adopts the same conformation as that of the parent compound [$Cu(Tr^{Mes,Me})]_2$: κ^3-S_2H (two thioxo groups and a [Cu···H−B] interaction).

2. Experimental Section

2.1. General Procedures. All solvents were commercially available and were stored under nitrogen on 4 Å molecular sieves (1−2 mm). Compounds [$Cu(Tr^{Mes,Me})]_2$, [$Cu(Tr^{Me,o-Py})]_2$, and [$Cu(Br^{Mes}pz^{o-Py})]_2$ were prepared as previously reported.[1] All other reagents were commercially available (Sigma-Aldrich) and were used as received. The ^{1}H and ^{13}C spectra were recorded on a Bruker Avance 300 spectrometer, and the ^{31}P NMR spectra were recorded on a Bruker AMX-400 spectrometer. ^{1}H and ^{13}C NMR spectra are referenced to residual solvent signals and $^{31}P\{^1H\}$ spectra are referenced to an external standard of 85% H_3PO_4. Two-dimensional experiments (^{1}H and ^{13}C HETCOR, COSY, and NOESY) were recorded using standard Bruker pulse sequences. The 2D-NOESY experiments were recorded using a mixing time (τ_m) of 0.6 s for **1**−**3**. Variable-temperature NMR experiments were recorded at 10 K intervals and performed in the 210−310 K range ($CDCl_3$ as solvent) for **1** and **2** and in the 200−310 K range (CD_2Cl_2 as solvent) for **3** in controlled-atmosphere valve NMR tubes. Two- and monodimensional FIDs were processed using the MestReC program suite.[6] Mass spectra were obtained with a Micromass ZMD spectrometer. The mixtures were analyzed in negative and positive ionization modes by direct perfusion in an ESI-MS interface; capillary = 3.0 kV, cone = 30 V, and extractor = 3 V. Infrared spectra were recorded using KBr pellets from 4000 to 400 cm^{-1} on a Perkin−Elmer FT-IR Nexus spectrometer. Elemental analyses (C, H, N) were performed with a Carlo Erba EA 1108 automated analyzer.

2.2. [$Ph_3PCu(Tr^{Mes,Me}$)] (1). [$Cu(Tr^{Mes,Me})]_2$ (211 mg, 0.137 mmol) and triphenylphosphine (81 mg, 0.309 mmol) were mixed in chloroform (6 mL). The solution was stirred for 1 h and then hexane (about 10 mL) was added until a minimum amount of precipitate formed, which was filtered and removed. Hexane in excess was added to the solution, giving rise to the formation of colorless microcrystals, which were filtered, washed with hexane, vacuum-dried, and collected (85 mg, 0.082 mmol, 30%). IR (KBr pellet, cm^{-1}): 3050 w, 2997 w, 2968 w, 2920 w, 2858 w, 2492 w br, [ν(BH)], 1609 w, 1580 m, 1488 m, 1419 s, 1369 s, 1325 s, 1301 s, 1275 s, 1172 w, 1153 w. ^{1}H NMR (300 MHz, $CDCl_3$): δ 1.73 (s, 9H, CH_3 Mes. ortho), 2.03 (s, 18H, CH_3 Mes. ortho; CH_3 triazole), 2.38 (s, 9H, CH_3 para), 5.07 (br, 1H, BH), 6.98 (s, 3H, CH Mes.), 6.99 (s, 3H, CH Mes.), 7.06 (m, 6H, CH, PPh_3 meta), 7.21 (m, 9H, CH, PPh_3 ortho and para).$^{13}C\{^1H\}$ NMR (75 MHz, $CDCl_3$): δ 11.17 (CH_3 Mes. ortho/CH_3 triazole), 18.14 (CH_3 Mes. ortho/CH_3 triazole), 18.62 (CH_3 Mes. ortho), 21.20 (CH_3 Mes. para), 127.7 (d, J_{CCCP} = 8.8 Hz, CH PPh_3 meta), 128.6 (s, CH PPh_3 para), 129.24 (CH Mes.), 129.49 (CH Mes.), 130.06 (C quat.), 133.85 (d, J_{CCP} = 14.3 Hz, CH PPh_3 ortho), 134.48 (d, J_{CP} = 25.7 Hz, C quat. PPh_3), 136.17 (C quat.), 136.73 (C quat.), 139.17 (C quat.), 148.20 (C quat.), 167.66 (C=S).$^{31}P\{^1H\}$ NMR (160 MHz, $CDCl_3$): δ −9.7 (s br). Anal. Calcd for $C_{54}H_{58}N_9S_3BCuP$ (1134.62): C, 62.69; H, 5.65; N, 12.18. Found: C, 62.12; H, 5.21; N, 11.91. Colorless crystals suitable for X-ray structure determination were obtained from a chloroform/hexane solution, [$Ph_3PCu(Tr^{Mes,Me})]_2$·$4CHCl_3$ (**1a**).

2.3. [$Ph_3PCu(Tr^{Me,o-Py}$)] (2). [$Cu(Tr^{Me,o-Py})]_2$ (81 mg, 0.062 mmol) and triphenylphosphine (34 mg, 0.130 mmol) were mixed in dichloromethane (10 mL). The solution was stirred for 1 h and then concentrated in a vacuum to about 5 mL of volume. A pale yellow product was precipitated by the addition of hexane. It was filtered, washed with hexane, vacuum-dried, and collected (80 mg, 0.088 mmol, 71%). IR (KBr pellet, cm^{-1}): 3050 w, 2498 w [ν-(BH)], 1589 m, 1478 s, 1455 m, 1434 m, 1411 s, 1341 s, 1216 m, 1084 m. ^{1}H NMR (300 MHz, $CDCl_3$): δ 3.98 (s, 9H, CH_3), 5.15 (s br, 1H, BH), 7.31 (m, 12H, CH py (3H) and CH PPh_3 meta and para (9H)), 7.59 (m, 6H, CH PPh_3 ortho), 7.73 (t, J = 7.2 Hz, 3H, CH py), 8.15 (d, J = 7.8 Hz, 3H, CH py), 8.63 (d, J = 4.2 Hz, 3H, CH py).^{13}C NMR (75 MHz, $CDCl_3$): δ 33.34 (CH_3 triazole), 124.07 (CH py), 128.28 (d, J_{CCCP} = 7.3 Hz, CH PPh_3 meta), 129.30 (CH PPh_3 para), 133.80 (d, J_{CCP} = 15.2 Hz, CH PPh_3 ortho), 136.61 (CH py), 147.24 (C quat.), 148.48 (CH py), 149.11 (C quat.), 169.95 (C=S).^{31}P NMR (160 MHz, $CDCl_3$): δ −5.0 (s br). Anal. Calcd

(3) (a) Fielding, L. *Tetrahedron* **2000**, *56*, 6151−6170. The NMR titration technique applied to transition-metal complexes can be found in the following references: (b) Wong, W. W. H.; Curiel, D.; Cowley, A. R.; Beer, P. D. *J. Chem. Soc., Dalton Trans.* **2005**, 774−781. (c) Wong, W. W. H.; Curiel, D.; Lai, S.-W.; Drew, M. G. B.; Beer, P. D. *J. Chem. Soc., Dalton Trans.* **2005**, 359−364. (d) Chartres, J. D.; Groth, A. M.; Lindoy, L. F.; Meehan, G. V. *J. Chem. Soc., Dalton Trans.* **2002**, 371−376. (e) Badura, D.; Vahrenkamp, H. *Inorg. Chem.* **2002**, *41*, 6020−6027. (f) Yang, G.; Miao, R.; Li, Y.; Hong, J.; Zhao, C.; Guo, Z.; Zhu, L. *J. Chem. Soc., Dalton Trans.* **2005**, 1613−1619. (g) Pescitelli, G.; Di Bari, L.; Salvatori, P. *Organometallics* **2004**, *23*, 4223−4229. (h) Tamm, M.; Kunst, A.; Bannenberg, T.; Herdtweck, E.; Schmid, R. *Organometallics* **2005**, *24*, 3163−3171. In this reference, NMR titration is used despite the isotropic shift: (i) Riviere, C.; Nierlich, M.; Ephritikhine, M.; Madic, C. *Inorg. Chem.* **2001**, *40*, 4428−4435.

(4) (a) Loeb, S. J.; Shimizu, G. K. H. *Inorg. Chem.* **1993**, *32*, 1001−1006. (b) de Groot, B.; Giesbrecht, G. R.; Loeb, S. J.; Shimizu, G. H. *Inorg. Chem.* **1993**, *30*, 177−182. (c) Loeb, S. J.; Shimizu, G. K. H. *Chem. Commun.* **1991**, 1119−1121. (d) Orhenberg, C.; Saleem, M. M.; Riordan, C. G.; Yap, G. P. A.; Verma, A. K.; Rheingold, A. L. *Chem. Commun.* **1996**, 1081−1082. (e) Ohrenberg, C.; Liable-sands, L. M.; Rheingold, A. L.; Riordan, C. G. *Inorg. Chem.* **2001**, *40*, 4276−4283.

(5) Lobbia, G. G.; Pettinari, C.; Santini, C.; Somers, N.; Skelton, B. W.; White, A. H. *Inorg. Chim. Acta* **2001**, *319*, 15−22.

(6) Cobas, J. C.; Sardina, F. J. *MestRe-C: A Software Package for Desktop Computers*; *Concepts Magn. Reson.* **2003**, *19A*, 80−96; http://www.mestrec.com/.

Table 1. Summary of X-ray Crystallographic Data for **1a**, **2a**, and **4**

	1a	**2a**	**4**
empirical formula	$C_{58}H_{62}BCl_{12}CuN_9PS_3$	$C_{45}H_{38}BcuN_{13}OPS_3$	$C_{56}H_{106}B_2Cl_{12}Cu_2N_{22}S_8$
formula weight	1512.07	978.38	1918.21
color, habit	colorless, block	colorless, block	colorless, block
cryst size (mm^3)	0.35 × 0.30 × 0.15	0.35 × 0.25 × 0.18	0.45 × 0.20 × 0.10
cryst syst	triclinic	triclinic	monoclinic
space group	$P\bar{1}$	$P\bar{1}$	$P2_1/c$
a (Å)	12.328(1)	10.573(1)	19.682(8)
b (Å)	12.901(1)	13.571(1)	17.139(8)
c (Å)	24.666(2)	38.381(2)	32.789(9)
α (deg)	77.466(1)	106.265(2)	90
β (deg)	79.834(1)	97.971(2)	97.26(2)
γ (deg)	75.178(1)	104.757(2)	90
V ($Å^3$)	3671.5(5)	2384.9(4)	10972(7)
Z	2	2	4
T (K)	293	293	245
ρ_{calcd} (Mg/m^3)	1.368	1.362	1.161
μ (mm^{-1})	0.883	0.673	4.906
θ range (deg)	1.66−27.02	1.64−27.07	3.31−64.68
no. of reflns/obsvd $F > 4\sigma(F)$	21770/7068	25981/4328	16374/5352
GOF	1.003	1.004	1.010
R1[a]	0.0551	0.0465	0.0850
wR2[a]	0.1123	0.0804	0.1655

[a] $R1 = \sum||F_o| - |F_c||/\sum|F_o|$, $wR2 = [\sum[w(F_o^2 - F_c^2)^2]/\sum[w(F_o^2)^2]]^{1/2}$, $w = 1/[\sigma^2(F_o^2) + (aP)^2 + bP]$, where $P = [\max(F_o^2,0) + 2F_c^2]/3$.

for $C_{42}H_{37}N_{12}S_3BCuP$ (911.35): C, 55.35; H, 4.09; N, 18.44. Found: C, 54.77; H, 4.13; N, 17.97. Colorless crystals were grown by slow evaporation from a dimethylformamide solution, $[Ph_3PCu(Tr^{Me,o-Py})]\cdot$DMF (**2a**).

2.4. [Ph$_3$PCu(Br^{Mes,Me}pz^{o-Py})] (3). Triphenylphosphine (21 mg, 0.080 mmol) was added to a dichloromethane solution (5 mL) of $[Cu(Br^{Mes,Me}pz^{o-Py})]_2$ (50 mg, 0.036 mmol). After 30 min of stirring, the volume was reduced to about 1 mL under reduced pressure. A bright yellow product was precipitated by the addition of an excess of hexane (ca. 10 mL). The product was filtered, washed with hexane, vacuum-dried, and collected (24 mg, 0.025 mmol, 35%). IR (KBr pellet, cm^{-1}): 3048 w, 3004 w, 2963 w, 2919 w, 2854 w, 2471 w br [ν(BH)], 1609 w, 1592 w, 1568 w, 1488 m, 1434 s, 1414 s, 1364 m, 1325 m, 1263 s, 1199 m, 1094 s, 1017 s. ^{1}H NMR (300 MHz, 298 K, CD_2Cl_2): δ 1.97 (s, 12H, CH_3), 2.05 (s, 6H, CH_3), 2.38 (s, 6H, CH_3), 6.81 (br, 1H, CH py), 6.87 (d, J = 2.1 Hz, 1H, CH pyrazole), 7.05 (s, 2H, CH arom. Mes.), 7.07 (s, 2H, CH arom. Mes.), 7.32 (m, 16H, CH PPh_3 (15H) and CH py), 7.63 (br, 1H, CH py), 8.16 (br, 1H, CH py), 8.27 (br, 1H, CH py). ^{31}P NMR (160 MHz, 298 K, $CDCl_3$): δ −2.4 (br). Anal. Calcd for $C_{50}H_{50}N_9S_2BCuP$ (946.45): C, 63.45; H, 5.32; N, 13.32. Found: C, 63.12; H, 5.62; N, 13.23.

2.5. [((NH$_2$)$_2$CS)Cu(Tr^{Mes,Me})]·3CH$_2$Cl$_2$ (4). Colorless crystals of $[(NH_2)_2CSCu(Tr^{Mes,Me})]$ were obtained from a hexane/dichloromethane solution (1:1 v/v) by mixing $[Cu(Tr^{Mes,Me})]_2$ (50 mg, 0.032 mmol) and an excess of Tu (14 mg, 0.184 mmol). The crystals were filtered, vacuum-dried, and collected (20 mg, 0.023 mmol, 35%). IR (KBr pellet, cm^{-1}): 3381 m br, 3301 m br, 3184 m br, 3014 m, 2959 w, 2920 w, 2855 w, 2481 w, 2410 w, 1609 s, 1576 m, 1488 m, 1406 s, 1374 s, 1326 s, 1301 s, 1274 m, 1172 m, 1144 m, 1013 m, 852 w. ^{1}H NMR (300 MHz, 298 K, CD_2Cl_2): δ 1.95 (s, 18H, CH_3), 2.03 (s, 9H, CH_3), 2.32 (s, 9H, CH_3), 6.43 (s, br, 4H, NH_2), 6.97 (s, 6H, CH Mes.).^{13}C{^{1}H} NMR (75 MHz, CD_2Cl_2): δ 11.45 (CH_3), 18.00 (CH_3), 21.29 (CH_3), 129.64 (CH Mes.), 130.22 (C quat.), 136.53 (C quat.), 140.20 (C quat.), 148.96 (C quat.), 168.05 (C═S), 182.63 (C═S Tu). Anal. Calcd for $C_{37}H_{47}N_{11}S_4BCu$ (848.46): C, 52.38; H, 5.51; N, 17.91. Found: C, 52.42; H, 5.48; N, 18.22.

2.6. X-ray Crystallography. A summary of data collection and structure refinement for $[Ph_3PCu(Tr^{Mes,Me})]\cdot 5CHCl_3$ (**1a**), $[Ph_3PCu(Tr^{Me,o-Py})]\cdot$DMF (**2a**), and $[(NH_2)_2CSCu(Tr^{Mes,Me})]\cdot 3CH_2Cl_2$ (**4**) is reported in Table 1. Single-crystal data were collected with a Bruker AXS Smart 1000 area detector diffractometer (Mo Kα; λ = 0.71073 Å) for **1a** and **2a** and with an Enraf Nonius CAD4 diffractometer (Cu Kα: λ = 1.54183 Å) equipped with an Oxford Cryosystems liquid nitrogen cryostream for **4** operating at 245 K. The crystal of **4** decomposed during the data collection, with a 40% intensity loss of the reference reflection. An absorption correction was applied using the program SADABS,[7] with transmission factors in the ranges 0.757−1.000 (**1a**) and 0.915−1.000 (**2a**) and using the method of Walker & Stuart[8] for **4** with minimum and maximum transmission factors of 0.816 and 1.000, respectively. The structures were solved by direct methods (SIR97)[9] and refined with the full-matrix least-squares method (SHELXL-97),[10] using the Wingx software package.[11] Non-hydrogen atoms were refined anisotropically; for **1a** and **2a**, the B-*H* hydrogen atoms were found and refined, whereas the remaining hydrogen atoms were placed at their calculated positions. In **4**, all the hydrogen atoms were placed at their calculated positions. In **1a**, three $CHCl_3$ molecules could be located from the difference Fourier map; two $CHCl_3$ solvent molecules were found disordered and were modeled with the SQUEEZE PLATON program.[12] The DMF molecule in **2a** was found disordered in two positions, with site occupancy factors of 0.57 and 0.43. In **4**, one CH_2Cl_2 solvent molecule was located from the difference Fourier map and two CH_2Cl_2 molecules were modeled with the SQUEEZE PLATON program. Ortep diagrams were prepared using the ORTEP-3 for Windows program.[13]

2.7. Quantum Chemical Calculations. All the calculations were performed with the Gaussian01 program suite.[14] Geometry opti-

(7) *Area-Detector Absorption Correction*; Siemens Industrial Automation, Inc.: Madison, WI, 1996.
(8) Walker, N.; Stuart, D. *Acta Crystallogr., Sect. A* **1983**, *39*, 158−166.
(9) Altomare, A.; Burla, M. C.; Camalli, M.; Cascarano, G. L.; Giacovazzo, C.; Guagliardi, A.; Moliterni, A. G. G.; Polidori, G.; Spagna, R. *J. Appl. Cryst.* **1999**, *32*, 115.
(10) Sheldrick, G. M. *SHELX97, Programs for Crystal Structure Analysis*, release 97-2; University of Göttingen: Göttingen, Germany, 1997.
(11) Farrugia, L. J. *J. Appl. Cryst.* **1999**, *32*, 837.
(12) Sluis, P. v.d.; Spek, A. L. *Acta Crystallogr., Sect. A* **1990**, *46*, 194.
(13) Farrugia, L. J. *J. Appl. Crystallogr.* **1997**, *30*, 565.

mizations were performed for the isomers of compounds **3** starting from geometries proposed on the basis of two- and monodimensional NMR experiments. The two-layer ONIOM technique[15] was employed. For the model system, all the mesityl groups and the methyl groups on the triazoline rings were approximated to hydrogen atoms, and the gradient-corrected hybrid density functional B3LYP[16,17] and double-ζ basis set LANL2DZ with Hay and Wadt effective core potential (ECP)[18,19] were used. A polarization d-function for the sulfur and phosphorus atoms was also added in the basis set. For the real system, Hartree−Fock with the LANL2MB basis set with Hay and Wadt ECP were used; the details of the partitioning scheme are given in the Supporting Information, Figure S16. Single-point energy calculations were performed for all compounds using the B3LYP density functional and the LANL2DZ basis set for copper and the 6-31G(d) basis set for the C, H, N, B, S, and P atoms. The energies of the various compounds do not include thermal or entropy corrections.

2.8. Stability Constant Calculations. Dilution experiments on $[Cu(Tr^{Mes,Me})]_2$, $[Cu(Tr^{Me,o-Py})]_2$, and $[Cu(Br^{Mes}pz^{o-Py})]_2$ were performed by collecting NMR spectra in the concentration range 1×10^{-2} to 1×10^{-4} M. The $[Cu(L)]_2/PPh_3$ systems were studied by titrating a 500 μL sample of $[Cu(L)]_2$ ($C \approx 1 \times 10^{-3}$ M, L = $Tr^{Mes,Me}$, $Tr^{Me,o-Py}$, $Br^{Mes}pz^{o-Py}$) with an ~0.1 M solution of PPh_3 (solvent: $CDCl_3$) The $[Cu(L)]_2$/Tu systems were studied by titrating an 800 μL sample of $[Cu(L)]_2$ ($C \approx 5 \times 10^{-3}$ M, L = $Tr^{Mes,Me}$, $Br^{Mes}pz^{o-Py}$) with an ~0.1 M solution of Tu. Twenty-five NMR spectra were collected in the Tu:$[Cu(Tr^{Mes,Me})]_2$ ratio range from 0 to 5 (1:1 v/v $CDCl_3$:MeOD solvent) and 12 NMR spectra were collected in the Tu:$[Cu(Br^{Mes}pz^{o-Py})]_2$ ratio range from 0 to 12.4 (1:1 v/v CD_2Cl_2:MeOD solvent). The solubility properties of $[Cu(Tr^{Me,o-Py})]_2$ and Tu prevented us from performing the NMR titration for this dinuclear complex. All sets of chemical shifts were treated simultaneously with the HypNMR 2004 program.[20] The $[Cu(L)]_2$/Py systems were studied by titrating a 500 μL sample of $[Cu(L)]_2$ ($C \approx 6 \times 10^{-3}$ M, L = $Tr^{Mes,Me}$, $Tr^{Me,o-Py}$, $Br^{Mes}pz^{o-Py}$) with a 0.1 M solution of Py (solvent: $CDCl_3$). Twenty NMR spectra were collected in the Py:$[Cu(Tr^{Mes,Me})]_2$ ratio range of 0 to 40 (solvent: $CDCl_3$); 13 NMR spectra were collected in the Py:$[Cu(Tr^{Me,o-Py})]_2$ ratio range of 0 to 64 (solvent: $CDCl_3$), and 10 NMR spectra were collected in the Py:$[Cu(Br^{Mes}pz^{o-Py})]_2$ ratio range of 0 to 40 (solvent: CD_2Cl_2). The titrations of $[Cu(Tr^{Me,o-Py})]_2$ and $[Cu(Br^{Mes}pz^{o-Py})]_2$ with Py were performed under nitrogen, because in air the solutions become dark green as a consequence of the Cu(I) → Cu(II) oxidation. All solutions were prepared by weight and used within 24 h. The distribution diagrams were calculated and plotted by the program HySS 2000.[21]

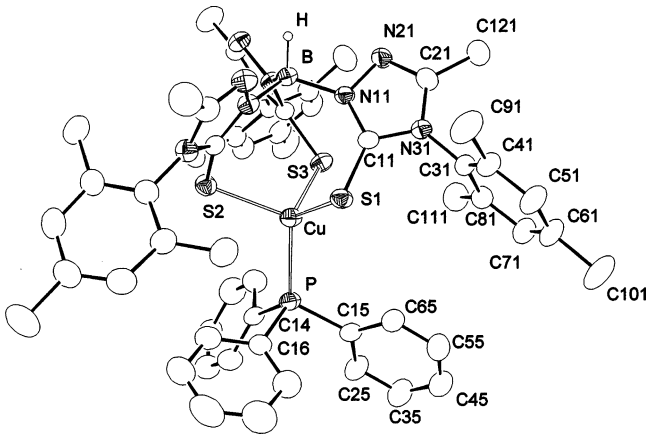

Figure 1. ORTEP drawing of **1a** at the 30% thermal ellipsoid probability level. Hydrogen atoms, except B-*H*, have been removed for clarity.

Scheme 1

$[Cu(Tr^{Mes,Me})]_2 + 2\ PPh_3 \xrightarrow{CHCl_3,\ N_2} 2\ [Ph_3PCu(Tr^{Mes,Me})]$

$[Cu(Tr^{Me,o\text{-}Py})]_2 + 2\ PPh_3 \xrightarrow{CH_2Cl_2,\ N_2} 2\ [Ph_3PCu(Tr^{Me,o\text{-}Py})]$

$[Cu(Br^{Mes,Me}pz^{o\text{-}Py})]_2 + 2\ PPh_3 \xrightarrow{CH_2Cl_2,\ N_2} 2\ [Ph_3PCu(Br^{Mes,Me}pz^{o\text{-}Py})]$

3. Results and Discussion

To explore the stability/reactivity of dinuclear complexes $[Cu(L)]_2$ (L = $Tr^{Mes,Me}$, $Tr^{Me,o-Py}$, or $Br^{Mes,Me}pz^{o-Py}$), we reacted them with three different monodentate σ-donor ligands: PPh_3, Tu, and Py. All the reactions were monitored through ^1H NMR titrations to evaluate, where possible, the formation constants of the ternary complexes [DCu(L)] (D = PPh_3, Tu, or Py). The reactions with PPh_3 are quantitatively in line with the high K_f values and, accordingly, the $[PPh_3Cu(L)]$ complexes were isolated by reacting the appropriate $[Cu(L)]_2$ with PPh_3 in chlorinated hydrocarbons, Scheme 1. These compounds can also be obtained by a one-pot reaction between $[Cu(CH_3CN)_4]BF_4$, LiL, and PPh_3. The products are colorless (**1**) or pale yellow (**2**−**3**) air-stable solids. The K_f of complexes [TuCu(L)] and [PyCu(L)] are much lower, and in some cases, especially when titrating with Py, they could not be determined (vide infra). Because of the low K_f values, we could not isolate the complexes from a 1:2 mixture of $[Cu(L)]_2$ and Tu or Py. However, colorless crystals of $[TuCu(Tr^{Mes,Me})]$ were obtained from a hexane:dichloromethane solution of $[Cu(Tr^{Mes,Me})]_2$ and Tu in a 1:6 ratio.

3.1. Molecular Structures. Essentially, the molecular structures of **1a** and **2a** (Figures1 and 2) present an equivalent type of copper(I) coordination. Selected bond lengths and angles are reported in Tables 2 and 3. The metal exhibits a tetrahedral geometry bound by a tridentate ligand (κ^3-S_3) and

(14) Frisch, M. J.; Trucks, G. W.; Schlegel, H. B.; Scuseria, G. E.; Robb, M. A.; Cheeseman, J. R.; Zakrzewski, V. G.; Montgomery, J. A., Jr.; Kudin, K. N.; Burant, J. C.; Millam, J. M.; Stratmann, R. E.; Tomasi, J.; Barone, V.; Mennucci, B.; Cossi, M.; Scalmani, G.; Rega, N.; Iyengar, S.; Petersson, G. A.; Ehara, M.; Toyota, K.; Nakatsuji, H.; Adamo, C.; Jaramillo, J.; Cammi, R.; Pomelli, C.; Ochterski, J.; Ayala, P. Y.; Morokuma, K.; Salvador, P.; Dannenberg, J. J.; Dapprich, S.; Daniels, A. D.; Strain, M. C.; Farkas, O.; Malick, D. K.; Rabuck, A. D.; Raghavachari, K.; Foresman, J. B.; Ortiz, J. V.; Cui, Q.; Baboul, A. G.; Clifford, S.; Cioslowski, J.; Stefanov, B. B.; Liu, G.; Liashenko, A.; Piskorz, P.; Komaromi, I.; Gomperts, R.; Martin, R. L.; Fox, D. J.; Keith, T.; Al-Laham, M. A.; Peng, C. A.; Nanayakkara, A.; Challacombe, M.; Gill, P. M. W.; Johnson, B.; Chen, W.; Wong, M. W.; Andres, J. L.; Gonzalez, C.; Head-Gordon, M.; Replogle, E. S.; Pople, J. A. *Gaussian01*, revision B.01; Gaussian, Inc.: Pittsburgh, PA, 2001.
(15) (a) Humbel, S.; Sieber, S.; Morokuma, K. *J. Chem. Phys*. **1996**, *105*, 1959−1967. (b) Svensson, M.; Humbel, S.; Froese, R. D. J.; Matsubara, T.; Sieber, S.; Morokuma, K. *J. Phys. Chem.* **1996**, *100*, 19357−19363. (c) Dapprich, S.; Komaromi, I.; Byun, K. S.; Morokuma, K.; Frisch, M. J. *J. Mol. Struct. (THEOCHEM)* **1999**, *461*−*462*, 1−21.
(16) Becke, A. D. *Phys. Rev.* A **1988**, *38*, 3098.
(17) Becke, A. D. *J. Chem. Phys.* **1993**, *98*, 5648.
(18) Hay, P. J.; Wadt, W. R. *J. Chem. Phys.* **1985**, *82*, 299.
(19) Wadt, W. R.; Hay, P. J. *J. Chem. Phys.* **1985**, *82*, 284.
(20) Frassineti, C.; Ghelli, S.; Gans, P.; Sabatini, A.; Moruzzi, M. S.; Vacca, A. *Anal. Biochem*. **1995**, *231*, 374−382.
(21) Alderighi, L.; Gans, P.; Ienco, A.; Peters, D.; Sabatini, A.; Vacca, A. *Coord. Chem. Rev*. **1999**, *184*, 311−318.

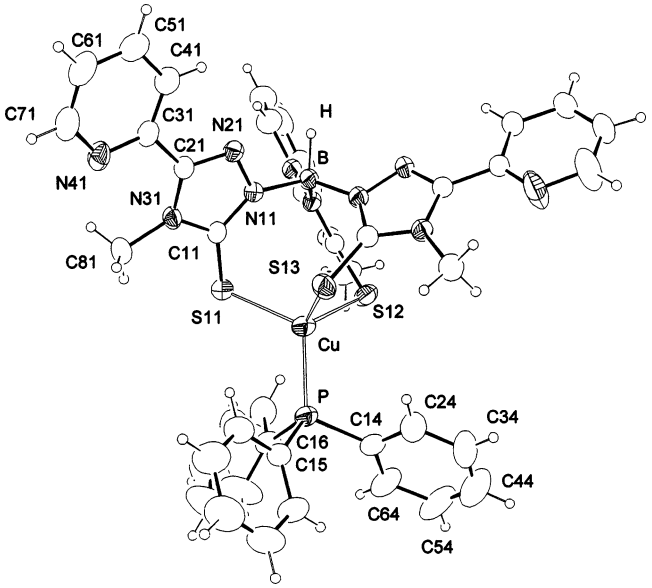

Figure 2. ORTEP drawing of **2a** at the 30% thermal ellipsoid probability level.

Table 2. Selected Bond Lengths (Å) and Angles (deg) for **1a**

Cu−S(1)	2.379(5)	B−N(12)	1.539(5)
Cu−S(2)	2.383(1)	B−N(13)	1.547(4)
Cu−S(3)	2.372(1)	C(11)−S(1)	1.692(3)
Cu−P	2.243(1)	C(12)−S(2)	1.699(3)
B−H	1.04(3)	C(13)−S(3)	1.697(4)
B−N(11)	1.549(5)		
S(1)−Cu−S(2)	107.03(4)	N(11)−B−N(12)	112.8(3)
S(1)−Cu−S(3)	105.77(3)	N(11)−B−N(13)	110.4(3)
S(2)−Cu−S(3)	102.39(4)	N(12)−B−N(13)	113.3(3)
S(1)−Cu−P	112.48(4)	N(11)−B−H	105(2)
S(2)−Cu−P	111.53(4)	N(12)−B−H	109(2)
S(3)−Cu−P	116.75(4)	N(13)−B−H	105(2)

Table 3. Selected Bond Lengths (Å) and Angles (deg) for **2a**

Cu−S(11)	2.352(1)	B−N(12)	1.554(4)
Cu−S(12)	2.363(1)	B−N(13)	1.559(4)
Cu−S(13)	2.343(1)	C(11)−S(11)	1.700(3)
Cu−P	2.220(1)	C(12)−S(12)	1.699(3)
B−H	1.14(2)	C(13)−S(13)	1.697(3)
B−N(11)	1.553(4)		
S(11)−Cu−S(12)	105.22(4)	N(11)−B−N(12)	112.2(3)
S(11)−Cu−S(13)	106.73(4)	N(11)−B−N(13)	113.2(3)
S(12)−Cu−S(13)	108.58(4)	N(12)−B−N(13)	111.5(3)
S(11)−Cu−P	114.59(4)	N(11)−B−H	106(1)
S(12)−Cu−P	107.65(4)	N(12)−B−H	107(1)
S(13)−Cu−P	113.62(4)	N(13)−B−H	107(1)

by a terminal PPh_3 with an overall coordination of the type S_3P. Both complexes present noncrystallographic C_3 symmetry. The Cu−P bond lengths (2.243(1) Å, **1a**; 2.220(1) Å, **2a**) are significantly shorter than the Cu−S bond distances (2.372(1)−2.385(1) Å, **1a**; 2.343(2)−2.363(1) Å, **2a**) and they are in accordance with the Cu−S and Cu−P separations reported for [R_3PCuTm)] (R = m-tolyl, p-tolyl)[5] and for the complexes with κ^3-S_3 thioether ligands.[4a−e] The Cu−P bond distance may be used as a rough index of the donor ability of the tridentate ligand located on the opposite side of the phosphine. In fact, the Cu−P bond lengths found in the (κ^3-S_3)-thioether/thioxoCuPR_3 compounds are longer (d_{mean} = 2.218(4) Å) than the ones reported for [R_3PCu(Tp)] (Tp = hydrotris(pyrazolyl)borato; R = aryl, alchyl) complexes (d_{mean} = 2.172(4) Å), in which the Tp is κ^3-N_3 coordinated.[22] This is in accordance with a more-pronounced donor ability of the sulfur donor ligands with respect to the nitrogen ones, resulting in a lengthening of the Cu−P distance. The only exception is represented by two [PPh_3Cu(Tp)] complexes that present bulky substituents on Tp (CF_3[23] and *p-tert*-butylphenyl[24]) that points toward the PPh_3 and may limit its approach to the copper [*d*(Cu−P) = 2.219(1) Å]. **1a** and **2a** exhibit the same coordinative environment, despite the fact that ligands $Tr^{Mes,Me}$ and $Tr^{Me,o-Py}$ present different substituents on the triazoline rings with different steric hindrance (methyl, piridyl, and mesityl groups). However, the S−Cu−S bond angles in **1a** (102.39(4)−107.03(4)°) are significantly smaller than the S−Cu−P bond angles (111.53(4)−116.75(4)°), whereas **2a** presents a more-regular tetrahedral geometry (S−Cu−S = 105.22(4)−108.58(4)°; S−Cu−P = 107.65(4)−114.59(4)°). This may be the result of the more-pronounced steric hindrance determined by the mesityl groups of $Tr^{Mes,Me}$, which limit the approach of the triphenylphosphine to the metal center. The pyridine fragments of the $Tr^{Me,o-Py}$ ligand are not participating in the metal coordination through the $N_{triazoline}-N_{pyridine}$ chelate system, as was proposed for one of the isomers of parent compound $[Cu(Tr^{Me,o-Py})]_2$.[1] When compared with the present structure, the pyridine coordination would imply a rotation of the pyridine ring with respect to the triazoline ring of ca. 180° and the displacement of two donor atoms from the copper(I) coordination. The preference of copper(I) for donor groups such as the C═S and phosphines eventually leads to a definite and rigid S_3P coordination environment, as evidenced by the nonfluxional behavior of **2** in $CDCl_3$ (vide infra).

The Ortep diagram of compound **4** is reported in Figure 3 and selected bond distances and angles in Table 4. In the unit cell, two independent complex molecules exhibiting the same molecular structure are present. The metals show a tetrahedral geometry bound by a tridentate ligand (κ^3-S_2H) and by a Tu with an $S_2S'H$ overall coordination. One of the three thioxo groups of the ligand is not bound to the metal. The ligand adopts the same conformation as that observed for dinuclear parent compound $[Cu(Tr^{Mes,Me})]_2$, with the B−H moiety pointing toward the metal. Even though the X-ray data were collected at low temperature, some crystal decomposition occurred, which affected the quality of the data. The B−H hydrogens could not be located from the difference Fourier map and were placed in their calculated

(22) (a) Kitajima, N.; Koda, T.; Hashimoto, S.; Kitagawa, T.; Moro-oka, Y. *J. Am. Chem. Soc.* **1991**, *113*, 5664−5671. (b) Gioia Lobbia, G.; Pettinari, C.; Marchetti, F.; Bovio, B.; Cecchi, P. *Polyhedron* **1996**, *15*, 881−890. (c) Gioia Lobbia, G.; Pettinari, C.; Santini, C.; Colapietro, M.; Cecchi, P. *Polyhedron* **1997**, *16*, 207−215. (d) Gioia Lobbia, G.; Pellei, M.; Pettinari, C.; Santini, C.; Skelton, B. W.; Somers, N.; White, A. H. *J. Chem. Soc., Dalton Trans.* **2002**, 2333−2340. (e) Pellei, M.; Pettinari, C.; Santini, C.; Skelton, B. W.; Somers, N.; White, A. H. *J. Chem. Soc., Dalton Trans.* **2000**, 3416−3424. (f) Gioia Lobbia, G.; Hanna, J. V.; Pellei, M.; Pettinari, C.; Santini, C.; Skelton, B. W.; White, A. H. *J. Chem. Soc., Dalton Trans.* **2004**, 951−958. (g) Pellei, M.; Gioia Lobbia, G.; Santini, G.; Spagna, R.; Cavalli, M.; Fedeli, D.; Falcioni, G. *J. Chem. Soc., Dalton Trans.* **2004**, 2822−2828.

(23) Rasika Dias, H. V.; Jin, W.; Kim, H.-J.; Lu, H.-L. *Inorg. Chem.* **1996**, *35*, 2317−2328.

(24) Conry, R. R.; Ji, G.; Tipton, A. A. *Inorg. Chem.* **1999**, *38*, 906−913.

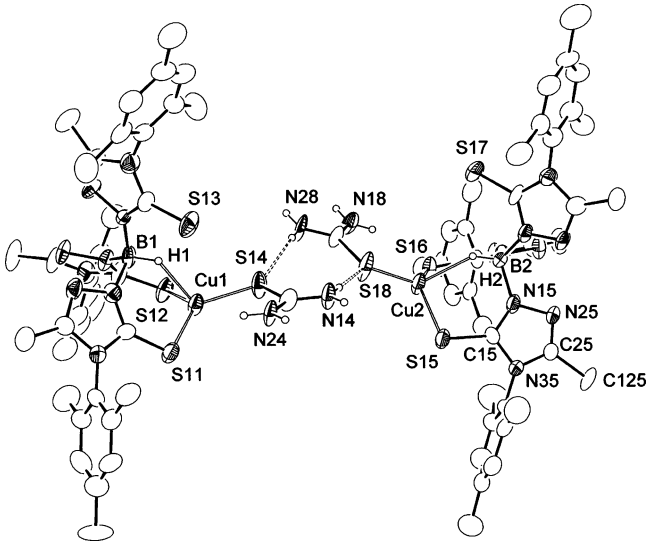

Figure 3. ORTEP drawing of **4** at the 30% thermal ellipsoid probability level. Hydrogen atoms, except those of the B-*H* and N*H*$_2$ groups, have been removed for clarity.

Table 4. Selected Bond Lengths (Å) for **4**

Cu(1)−S(11)	2.264(3)	B(1)−N(13)	1.47(1)
Cu(1)−S(12)	2.281(2)	C(11)−S(11)	1.707(9)
Cu(1)−S(14)	2.221(3)	C(12)−S(12)	1.698(9)
Cu(1)−B(1)	2.91(1)	C(13)−S(13)	1.682(8)
B(1)−N(11)	1.57(1)	C(14)−S(14)	1.748(8)
B(1)−N(12)	1.56(1)		
Cu(2)−S(15)	2.288(3)	B(2)−N(17)	1.46(1)
Cu(2)−S(16)	2.260(3)	C(15)−S(15)	1.715(8)
Cu(2)−S(18)	2.223(3)	C(16)−S(16)	1.722(8)
Cu(2)−B(2)	2.93(1)	C(17)−S(17)	1.680(8)
B(2)−N(15)	1.60(1)	C(18)−S(18)	1.759(8)
B(2)−N(16)	1.54(1)		

positions. The interacting Cu−H(B) distances are 2.108 (Cu(1)−H(1)) and 2.152 Å (Cu(2)−H(2)), which are in accordance with three-center, two-electron [B−H···Cu] interactions for both independent molecules.[25] Accordingly, the metal sites exhibit a significant deviation from the plane defined by the three sulfur atoms (sum of angles at copper: 356.0(5)° for Cu(1) and 355.2(5)° for Cu(2)), and the distortion from planarity (0.262(1) Å for Cu(1) and 0.286(2) Å for Cu(2)) is directed toward the B−H group. This is in agreement with the Cu−H distance found in dinuclear complexes $[Cu(Tr^{Mes,Me})]_2$, $[Cu(Tr^{Me,o-Py})]_2$, and $[Cu(Tr^{Et,Me})]_2$[26] (*d*(Cu−HB) = 1.94(4)−2.29(3) Å). From the analysis of the bond distances involving the coordinated C═S, it appears that the Tu interacts more strongly with copper when compared to the thioxo groups of the ligand. In fact, the Cu−S_{Tu} bond distances are shorter (2.221(3)−2.223(3) Å) than the Cu−S_{ligand} bond lengths (2.260(3)−2.288(3) Å), and the C═S_{Tu} distances (1.748(8)−1.759(8) Å) are significantly longer than the C═S_{ligand} distances (1.680(8)−1.722(8) Å). All of the Tu hydrogen atoms are involved in an extensive net of hydrogen bonds (HB) that determine the formation of layers in the *ab* plane (Figure 4). The HBs can be classified in three types according to the HB acceptor: (1) NH···S intramolecular HB with a triazoline thioxo group as acceptor, (2) NH···N intermolecular HB with the triazoline nitrogen atoms as acceptors, and (3) NH···S intermolecular HB with the C═S_{Tu} as acceptor. The mesityl groups of the ligand $Tr^{Mes,Me}$ are pointing above and below these layers and determine the packing along the *c* crystallographic axis through hydrophobic interaction.

3.2. Computational Studies. Despite all attempts to crystallize compound **3**, we could not obtain suitable crystals for an X-ray structure analysis. For this reason, DFT calculations were employed to propose reasonable structures of **3** and explain the fluxional behavior observed in CD_2Cl_2 solution according to 2D NMR spectra, variable-temperature NMR experiments, and PPh_3 titration (vide infra). In Figure 5, the conformations and the relative energies of three isomers of **3** are reported, and in Table 5, their relevant geometric parameters are listed. The geometry optimizations were performed using initial geometries proposed on the basis of the NOESY spectrum (240 K), which suggests that the most-abundant species present in solution display the PPh_3 coordinated to copper. In the **3a**−**c** isomers, the metal presents a tetrahedral geometry but with the $Br^{Mes}pz^{o-Py}$ ligand in different conformations and different donor sets (S_2H for **3a** and S_2N for **3b**,**c**). According to the isomers' relative energies, the most stable species is isomer **3a**. The energy difference between the **3a** and **3b** isomers is 8.3 kJ/mol, which is in agreement with a possible equilibrium between the two species as evidenced by the NMR experiments. This energy difference also justifies the fact that the **3b** isomer is essentially undetected by the NMR experiments. The structural reorganization for the **3a** ↔ **3b** process involves an inversion of the ligand conformation, because in **3a**, the B−H group is bound to the metal (*d*(Cu−H) = 1.915 Å), whereas in **3b**, it points outward and the pirazole nitrogen atom enters the metal coordination, Scheme 3. The N(33) nitrogen atom in **3b** is directed toward the copper but is located at a noninteracting distance (3.320 Å). The overall change in the copper coordination for this process would be S_2HP ↔ S_2NP. The destabilization of the **3c** isomer with respect to **3b** (25.6 kJ/mol) is due to the pyridine conformation, which presents a C−H group that interferes with the metal and the C−H_{ortho} of the triphenylphosphine.

3.3. NMR Spectroscopy. ^{1}H, ^{13}C{H}, and ^{31}P{H} NMR spectra for the three complexes were recorded in $CDCl_3$ (**1** and **2**) and CD_2Cl_2 (**3**). The assignment of the methyl and aromatic protons for all compounds was possible through 2D experiments (NOESY, COSY, and ^{13}C and ^{1}H HETCOR). For **1** and **2**, only one set of ^{1}H and ^{13}C signals was detected for the three arms of the tripodal ligands, which is in accordance with the pseudo-C_3 symmetry exhibited by the complexes in the solid state. To determine whether these systems were subject to a fluxional behavior, we performed variable-temperature NMR spectroscopy experiments in $CDCl_3$ for **1** and **2** (210−310 K; see the Supporting Information). When the temperature was decreased, we observed a slight variation of the chemical shifts without coalescence of the signals, in agreement with a certain structural rigidity of the complexes in solution. This is also

(25) Crabtree, R. H. *The Organometallic Chemistry of the Transition Metals*; Wiley-Interscience: Hoboken, NJ, 2005.
(26) Careri, M.; Elviri, L.; Lanfranchi, M.; Marchio, L.; Mora, C.; Pellinghelli, M. A. *Inorg. Chem.* **2003**, *42*, 2109−2114.

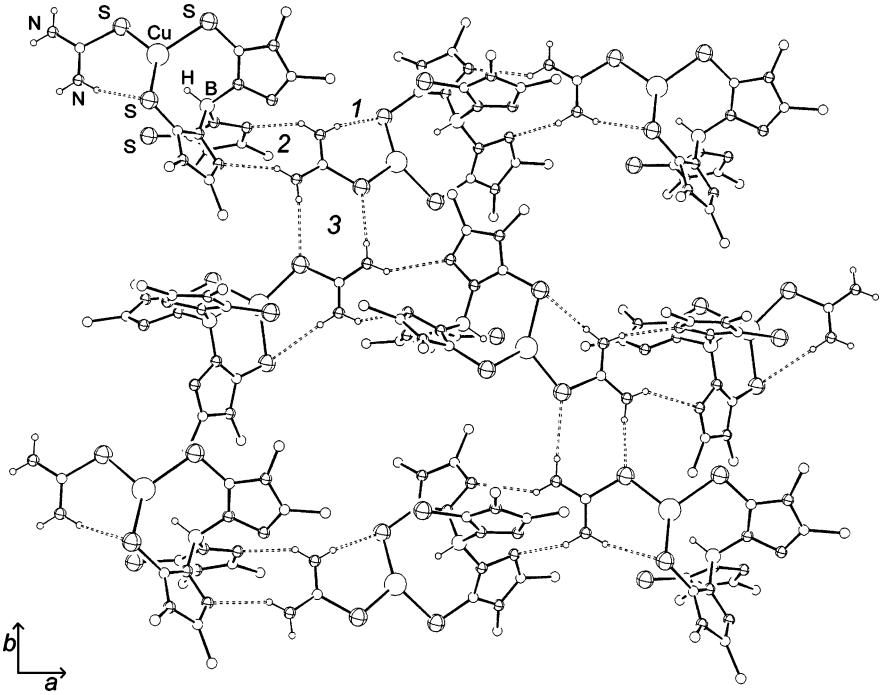

Figure 4. Crystal packing of **4** in the *ab* plane. Three types of hydrogen bonds are present. The mesityl groups and the hydrogen atoms (except the B-*H* and NH_2) have been removed for clarity.

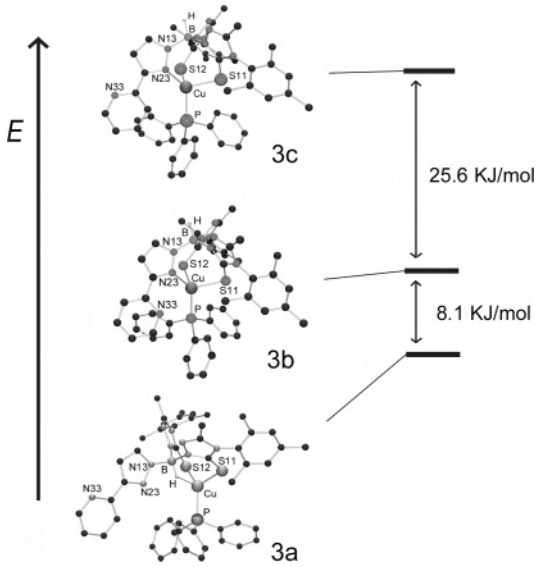

Figure 5. Calculated energy diagram for the **3a**−**c** isomers. Optimized geometries were obtained at the ONIOM b3lyp/lanl2dz-HF/lanl2mb level. Single-point energy calculations were performed with the b3lyp density functional and with the lanl2dz (Cu) and 6-31G(d) (other atoms) basis set.

Table 5. Calculated Bond Lengths (Å) and Angles (deg) for **3a**−**c**

	3a		
Cu−S(11)	2.425	B−H	1.204
Cu−S(12)	2.387	C(11)−S(11)	1.708
Cu−H	1.915	C(12)−S(12)	1.709
Cu−P	2.332		
S(11)−Cu−S(12)	114.70	S(12)−Cu−H	88.90
S(11)−Cu−H	90.22	S(11)−Cu−P	115.56
S(12)−Cu−P	126.06	H−Cu−P	109.07
	3b		
Cu−S(11)	2.446	B−H	1.194
Cu−S(12)	2.567	C(11)−S(11)	1.708
Cu−N(23)	2.079	C(12)−S(12)	1.701
Cu−P	2.356	Cu−N(33)	3.320
S(11)−Cu−S(12)	106.79	S(12)−Cu−N(23)	91.92
S(11)−Cu−N(23)	107.44	S(11)−Cu−P	107.88
S(12)−Cu−P	102.33	N(23)−Cu−P	135.85
	3c		
Cu−S(11)	2.505	B−H	1.193
Cu−S(12)	2.447	C(11)−S(11)	1.704
Cu−N(23)	2.092	C(12)−S(12)	1.706
Cu−P	2.363		
S(11)−Cu−S(12)	105.42	S(12)−Cu−N(23)	109.14
S(11)−Cu−N(23)	94.91	S(11)−Cu−P	104.54
S(12)−Cu−P	105.03	N(23)−Cu−P	134.15

evidenced by the NOESY spectra of **1** and **2**, which present cross peaks between the triphenylphosphine ortho and meta CH and the CH_3-mesityl groups (**1**) and the triazoline methyl groups (**2**), respectively, Scheme 2. This confirms that PPh_3 is bound to the metal and close to the $Tr^{Mes,Me}$ and $Tr^{Me,o-Py}$ ligands. Moreover, the pyridine rings of **2** are oriented with the nitrogen atoms toward the triazoline methyl groups, as evidenced by the cross peak between the H_a proton and the triazoline CH_3 (*e* protons), Scheme 2 and the Supporting Information, Figure S11. These data would confirm that the solution structures of **1** and **2** are equivalent to the solid state structures. On the other hand, compound **3** exhibits a fluxional behavior in CD_2Cl_2 solution, as derived from variable-temperature NMR experiments (200−310 K), Figure 6. The assignment of the signals at 240 K was possible through a COSY experiment, Fig. S14. The major species evident at 240 K is in equilibrium with a second species present in a small concentration, and its signals are very broad or covered by the major species signals. The NOESY spectrum recorded in CD_2Cl_2 at 298 K (above the coalescence temperature) presents a positive cross peak indicative of the fluxional behavior of the complex, which involves the H_a proton and another proton of a second species exhibiting a very broad signal at approximately 8.50 ppm,

Scheme 2

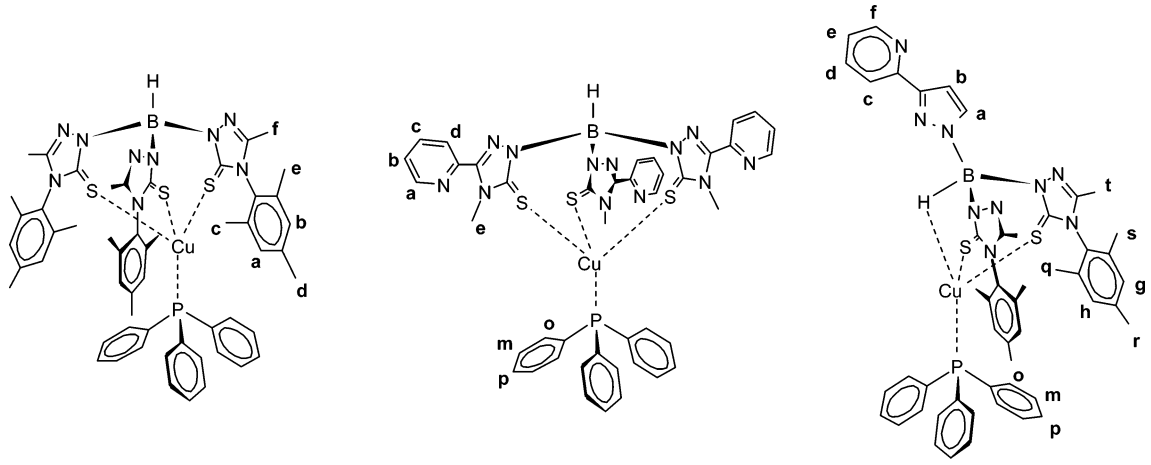

1 **2** **3a**

Scheme 3

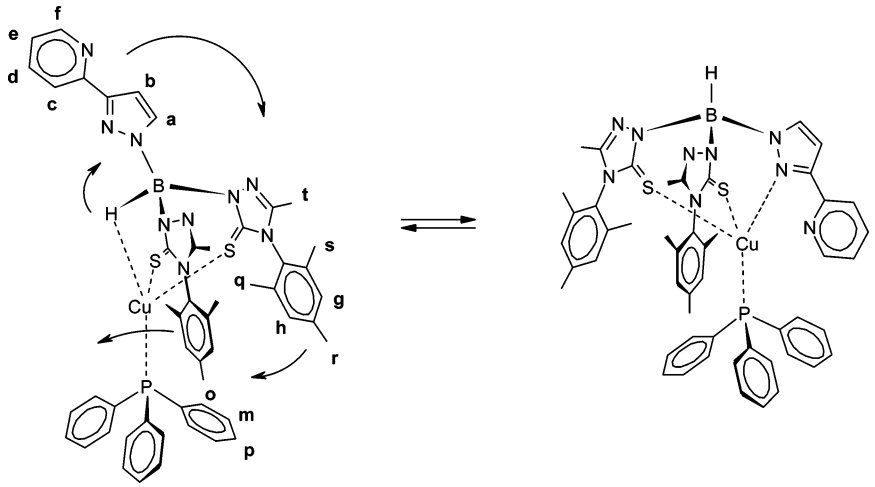

3a 3b

see the Supporting Information, Figure S15. Unfortunately, the remaining positive cross peaks arising from the dynamic process could not be detected. The NOESY spectrum recorded in CD_2Cl_2 at 240 K confirms the PPh_3 coordination to the metal because the ortho mesityl CH_3 groups of the $Br^{Mes,Me}pz^{o-Py}$ ligand and the ortho and meta triphenylphosphine protons give rise to negative cross peaks (Figure 7). This is in accordance with the **3a**−**c** geometries proposed on the basis of the calculations (Figure 5), as the minimum distances between the PPh_3−C*H* and the mesityl-CH_3 are 4.08 Å (**3a**), 2.78 Å (**3b**), and 2.69 Å (**3c**); unfortunately, this does not constitute a discriminating factor between them. However, the absence of the H_b−H_c and the H_f −PPh_3−C*H* cross peaks is in agreement with the **3a** and **3c** structures that display the pyridine N(33) pointing away from the metal and rules out the **3b** isomer as the major species present in solution at 240 K.

Dinuclear complexes $[Cu(Tr^{Mes,Me})]_2$, $[Cu(Tr^{Me,o-Py})]_2$, and $[Cu(Br^{Mes}pz^{o-Py})]_2$ were titrated with PPh_3, Tu, and Py in order to determine the K_f values for the ternary complexes Cu/L/PPh_3, Cu/L/Tu, and Cu/L/Py and gain insights concerning their stability/reactivity with respect to monodentate σ donors. The reaction with PPh_3 is complete after the addition of 2 equiv of PPh_3 with respect to $[Cu(L)]_2$. These data suggest that the K_f for the reaction $[Cu(L)]_2 + 2PPh_3 \rightarrow 2[PPh_3Cu(L)]$ is quite high but, under these experimental conditions, it is not possible to determine its value, because the titration goes to completeness when the $[Cu(L)]_2$:PPh_3 ratio is 1:2. Moreover, to confirm that the fluxional behavior of **3** occurs through a conformational rearrangement and not through a PPh_3 dissociative mechanism, we performed the titration of $[Cu(Br^{Mes}pz^{o-Py})]_2$ with PPh_3 up to a ratio of 1:10. The observation that the line shapes and line widths in the ^{1}H NMR spectrum did not change significantly supported the hypothesis of an equilibrium involving a molecular rearrangement within the $[PPh_3Cu(Br^{Mes}pz^{o-Py})]$ unit (**3a** ↔ **3b** equilibrium as proposed on the basis of the calculations, Scheme 3).

The ^{31}P chemical shifts may be used as an index of the ligand donor ability in complexes **1**−**3**. For complexes **1** and **2**, the ^{31}P δ are −9.7 and −5.0, respectively, whereas complex **3** presents a higher value (−2.4 ppm). This can be explained considering that for **1** and **2**, the ligands are coordinated to the metal through three C═S groups, hence

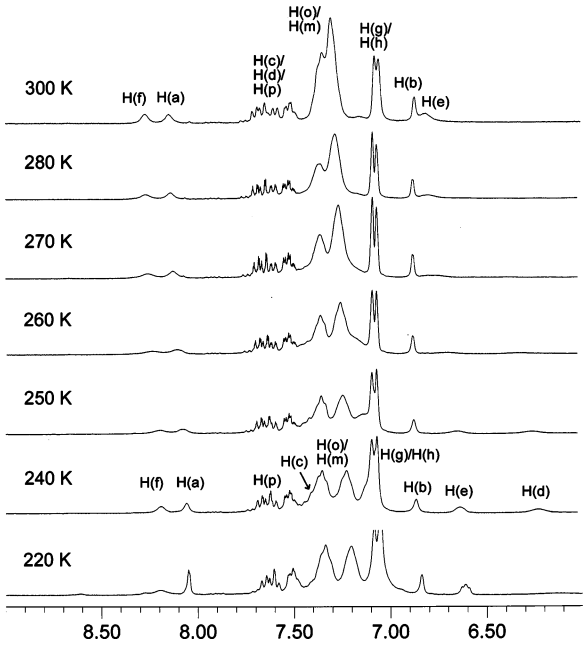

Figure 6. Temperature dependence of the ^{1}H NMR spectrum of **3** in CD_2Cl_2 (aromatic region). The attribution of the signals at 298 and 240 K was made according to the 2D experiments. The "/" refers to the undistinguishable signals of the major isomer.

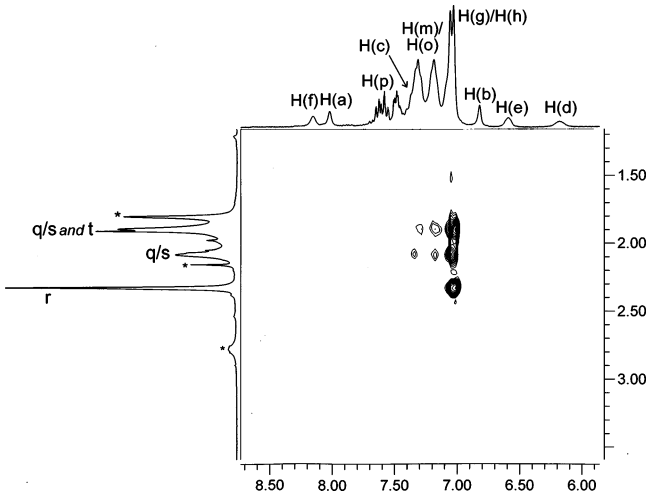

Figure 7. Aromatic and methyl regions of the NOESY NMR spectrum of **3** at 240 K in CD_2Cl_2. Solid lines denote negative cross peaks; The "/" refers to the undistinguishable signals of the major isomer. * = water and impurities. See Scheme 3 for signal attribution.

the more negative ^{31}P δ values and, specifically in **2**, the pyridine groups may exert some electron-withdrawing effect with respect to the mesityl groups of **1**, resulting in higher ^{31}P δ values. As far as **3** is concerned, from the calculated structure of the major species **3a**, the ligand $Br^{Mes,Me}pz^{o-Py}$ is bound to the metal with two C=S groups and a B−H group. This may be responsible for an overall minor donor ability of $Br^{Mes,Me}pz^{o-Py}$ with respect to the $Tr^{Mes,Me}$ and $Tr^{Me,o-Py}$ ligands, giving rise to a downfield shift of the ^{31}P signal.

More interesting is the titration of $[Cu(Tr^{Mes,Me})]_2$ and $[Cu(Br^{Mes}pz^{o-Py})]_2$ with Tu, because the reaction completion is reached at a higher Tu:$[Cu(L)]_2$ ratio. Moreover, the NMR titration clearly showed that equilibrium is under fast-exchange conditions above approximately 290 K; decreasing

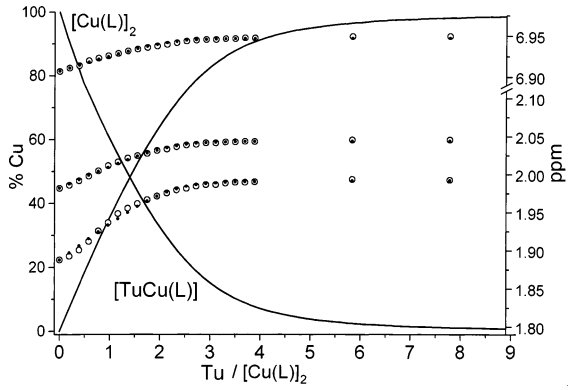

Figure 8. Distribution diagram (solid lines) and chemical shift values for the ^{1}H NMR titration of $[Cu(Tr^{Mes,Me})]_2$ with Tu in 1:1 v/v CD_3OD:CDCl. ○ = experimental chemical shifts, ● = calculated chemical shifts.

Scheme 4

$$2\,[Cu(L)] \rightleftharpoons [Cu(L)]_2 \qquad \beta Dim$$

$$[Cu(L)] + D \rightleftharpoons [DCu(L)] \qquad \beta$$

$$[Cu(L)]_2 + 2D \rightleftharpoons 2\,[DCu(L)] \qquad K_f$$

$$\log K_f = 2 \log \beta - \log \beta Dim$$

the temperature leads the systems to exhibit slow-exchange features with distinguishable signals of the [TuCu(L)] adducts and the dinuclear complexes. Unfortunately, an accurate determination of the coalescence temperature is difficult as a consequence of the overlapping of signals of $[Cu(L)]_2$ and [TuCu(L)] adducts, and no information could be obtained concerning the activation parameters. We studied the Tu/$[Cu(L)]_2$ system at a temperature above the coalescence (fast-exchange condition) by following the chemical shift variation as a function of Tu concentration using the curve-fitting procedure.[3a] According to the equilibria reported in Scheme 4, the stability constants of the $[Cu(L)]_2 + 2Tu = 2[TuCu(L)]$ equilibrium ($\log \beta$) can be calculated if the constant for the dimerization process $2[Cu(L)] = [Cu(L)]_2$ is known ($\log \beta$Dim). However, it can be demonstrated that if $\log \beta$Dim is high enough (i.e., [Cu(L)] is negligible), $\log \beta$ becomes independent from it. Dilution studies of the $[Cu(Tr^{Mes,Me})]_2$ and $[Cu(Br^{Mes}pz^{o-Py})]_2$ complexes in 1:1 v/v CD_3OD:CD_3Cl showed no dissociation of the dimers in the 1×10^{-2} to 1×10^{-4} M concentration range, so $\log \beta$Dim is expected to be quite high. Assuming that a 5% dissociation of the dimeric complex may occur but that it cannot be detected at the experimental concentration of 5×10^{-4} M (i.e., 5×10^{-5} M [Cu(L)]), $\log \beta$Dim would be >5.3. With this approximation ($\log \beta$Dim = 5.3), a calculated $\log \beta$ of 4.81(5) was determined. Finally, the $\log K_f$ value for the $[Cu(L)]_2 + 2Tu = 2[TuCu(L)]$ equilibrium resulted in 4.3(2) ($\log K_f = 2\log \beta - \log \beta$Dim). Calculations performed using a $\log \beta$Dim value higher than 5.3 led to the same $\log K_f$ value. For the $[Cu(Tr^{Mes,Me})]_2$ titration, the chemical shifts of the mesityl-*o*-CH_3 (ca. 1.9 ppm), triazolyl-CH_3 (ca. 2.0 ppm), and mesityl-CH (ca. 6.9 ppm) were taken into account to determine $\log \beta$, Figure 8. The same procedure was applied to the data of the NMR titration of $[Cu(Br^{Mes}pz^{o-Py})]_2$ with Tu. The calculations performed with the chemical shifts of

the mesityl-*o*-CH_3, the triazolyl-CH_3, and the mesityl-CH led to a log $K_f = 2.1(2)$. The stability of [TuCu(L)] with respect to the $[Cu(Tr^{Mes,Me})]_2$ dimer is thus 2.2 orders of magnitude higher than that for the $[Cu(Br^{Mes}pz^{o-Py})]_2$ dimer. With the β value independent of the dimerization constant βDim, its value takes into account the stability of the dimer, and this difference of 2 orders of magnitude directly reflects the tendency of the Tu to react preferentially with $[Cu(Tr^{Mes,Me})]_2$ over $[Cu(Br^{Mes}pz^{o-Py})]_2$. We attempted to evaluate the dependence of the K_f on the temperature according to the Van't Hoff analysis, to obtain information on ΔH^0 and ΔS^0. Unfortunately, both for the slow- and fast-exchange regimes, the $K_f(T)$ variations observed are well within the experimental error, thus providing no insights into the thermodynamic parameters for the reactions. Nevertheless, one may speculate that if the formation constant does not vary appreciably with the temperature, the ΔH^0 has to be small. As far as the $[Cu(Tr^{Mes,Me})]_2$/[TuCu($Tr^{Mes,Me}$)] system is concerned, for which the X-ray geometries are reported, this is in agreement with the equivalence of the coordination environment of copper in the parent dimer and in the Tu adduct. In fact, in both compounds, the metal exhibits the same type of donor atoms: three C=S groups and a Cu···H−B interaction.

Attempts to determine the β value for the competitive reaction [TuCu(L)] + PPh_3 = [PPh_3Cu(L)] + Tu were unsuccessful. In fact, even in the presence of an excess of a competitor such as Tu (Tu:$[Cu(L)]_2$ = 10:1) the reaction goes to completeness with 2 equiv of PPh_3 with respect to the dimer; no change in the spectra is observed when an excess of PPh_3 is added. With the limit of 5% free out of the total amount of PPh_3 present at the equilibrium by addition of 2 equiv of this ligand, we could determine that the log K_f for the reaction $[Cu(L)]_2 + 2PPh_3 = 2[PPh_3Cu(L)]$ should be >8.2 ([PPh_3Cu($Tr^{Mes,Me}$)]) and >7.2 ([PPh_3Cu($Br^{Mes}pz^{o-Py}$)]) (simulations performed with $C_{dimer} = 5 \times 10^{-3}$ M, $C_{Tu} = 25 \times 10^{-3}$ M). This value means that PPh_3 reacts at least 4 orders of magnitude more favorably than Tu with the studied dimers.

According to the ^{1}H NMR titrations, the only dimer that reacted with Py was $[Cu(Tr^{Mes,Me})]_2$, whereas for $[Cu(Tr^{Me,o-Py})]_2$ and $[Cu(Br^{Mes}pz^{o-Py})]_2$, a Py excess of 40-fold or 64-fold, respectively, did not give any reaction product. The $[Cu(Tr^{Mes,Me})]_2$/Py system was under the slow-exchange limit in the 220−340 K temperature range, and therefore the ratio between the integrals of the parent dimer and the Py adduct were used to determine the K_f for the reaction $[Cu(Tr^{Mes,Me})]_2 + 2Py = 2[PyCu(Tr^{Mes,Me})]$ (see the Supporting Information for the K_f equation under the slow-exchange limit). This procedure was hindered by the signal overlap of the $[Cu(Tr^{Mes,Me})]_2$ and [PyCu($Tr^{Mes,Me}$)] species, and the overlapping signals were treated using the deconvolution routine of the MestReC program. Moreover, the [PyCu($Tr^{Mes,Me}$)]:$[Cu(Tr^{Mes,Me})]_2$ ratio was temperature-dependent and ensured the possibility of extracting thermodynamic parameters from the $[Cu(Tr^{Mes,Me})]_2$/Py titration at different temperatures (260−305 K). The Van't Hoff analysis gave a ΔH^0 of -53.1 ± 2.8 kJ mol^{-1} and a ΔS^0 of -144 ± 24.7 J mol^{-1} K^{-1} (Figure 9). This exothermic reaction can

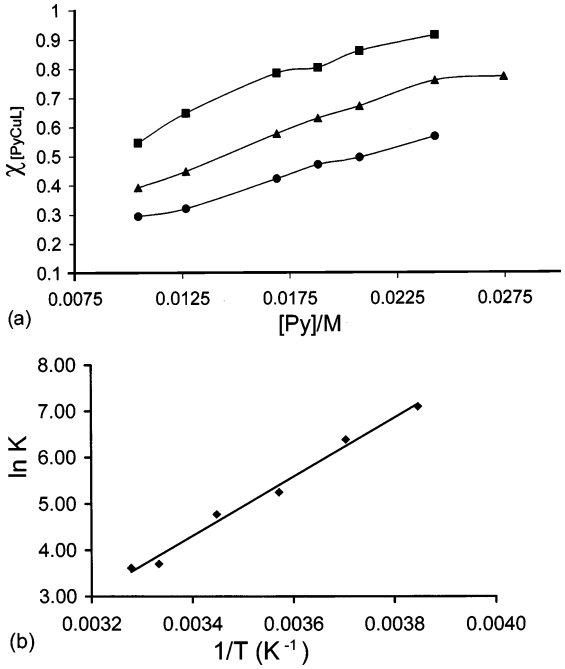

Figure 9. (**a**) Saturation plots reporting the molar fraction [PyCu(L)]/([PyCu(L)]+[Cu(L)]$_2$) with L = $Tr^{Mes,Me}$ obtained from the deconvolution procedure vs pyridine concentration at three representative temperatures. ■ = 270 K, ▲ = 290 K, ● = 305 K. (**b**) Van't Hoff plot: ln K = $-(\Delta H^0/R)/T + \Delta S^0/R$, $R = 8.3145$ J mol^{-1} K^{-1}, $T = 260-305$ K, experimental values (♦) and least-squares fit (−).

be explained by considering the different donor atoms involved in the copper(I) coordination in $[Cu(Tr^{Mes,Me})]_2$ and in [PyCu($Tr^{Mes,Me}$)]. In fact, a tentative assignment of the [PyCu($Tr^{Mes,Me}$)] molecular structure is the one in which the ligand behaves as in the PPh_3 adducts (with the B−H pointing away from the metal) and with a Py coordinated to the metal. This requires the $S_3H \rightarrow S_3N$ change in the coordination sphere for each metal in the dimer and it leads to the conclusion that the Cu···H−B interaction is weaker than the Cu···N(Py) one (Scheme 5).

4. Conclusions

The reactivity of dinuclear complexes $[Cu(L)]_2$ (L = $Tr^{Mes,Me}$, $Tr^{Me,o-Py}$, $Br^{Mes}pz^{o-Py}$) with monodentate ligands PPh_3, Tu, and Py (D) was investigated by means of NMR techniques. A summary of the K_f values of the [DCu(L)] adducts is shown in Table 6. $[Cu(Tr^{Mes,Me})]_2$ and $[Cu(Br^{Mes,Me}pz^{o-Py})]_2$ show a precise K_f trend that varies in the following order, $K_f([PPh_3Cu(L)]) \gg K_f([TuCu(L)]) > K_f([PyCu(L)])$. $[Cu(Tr^{Me,o-Py})]_2$ reacts quantitatively with PPh_3 but no appreciable reaction occurs, even with a large excess of Py (K_f([PyCu($Tr^{Me,o-Py}$)] undetermined), and the reaction of $[Cu(Tr^{Me,o-Py})]_2$ with Tu could not be studied because of the different solubility properties of the two species. The small values for K_f in the Py case are readily explained by considering the great affinity of copper(I) for sulfur and phosphorus ligands compared to that for nitrogen ones.[27]

(27) (a) Pearson, R. G. *J. Am. Chem. Soc.* **1963**, *85*, 3533−3539. (b) Pearson, R. G. *Inorg. Chem.* **1988**, *27*, 734−740. (c) Pearson, R. G. *Coord. Chem. Rev.* **1990**, *100*, 403−425.

Scheme 5

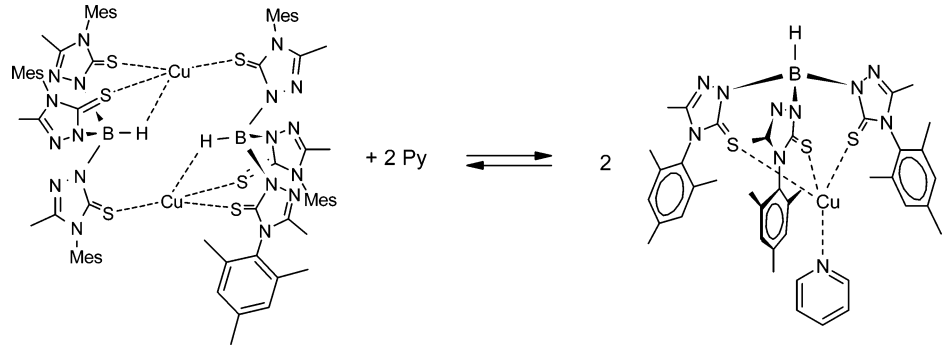

Table 6. Summary of the log K_f Values for the $[Cu(L)]_2 + 2D = 2[DCu(L)]$ Equilibria[a]

	PPh_3	Tu	Py
$[Cu(Tr^{Mes,Me})]_2$	>8.2[b] (300)	4.3(2)[e] (300)	1.6(1) (300)[g]
$[Cu(Tr^{Me,o-Py})]_2$	n.d.[c]	n.d.[c]	[h]
$[Cu(Br^{Mes}pz^{o-Py})]_2$	>7.2[d] (300)	2.1(2)[f] (300)	[h]

[a] Values in parenthesis are the reported temperatures (K). [b] 1:1 v/v $CDCl_3$:MeOD, determined from competitive reaction with Tu. [c] n.d. = not determined because of the different solubilities of Tu and $[Cu(Tr^{Me,o-Py})]_2$. [d] 1:1 v/v CD_2Cl_2:MeOD, determined from competitive reaction with Tu. [e] 1:1 v/v $CDCl_3$:MeOD. [f] 1:1 v/v CD_2Cl_2:MeOD. [g] $CDCl_3$, experimental value. [h] No reaction occurred using a large excess of Py.

The X-ray molecular structures of the complexes $[PPh_3Cu(Tr^{Mes,Me})]$ and $[PPh_3Cu(Tr^{Me,o-Py})]$ are reported and show the same tetrahedral copper(I) environment (κ^3-S_3 ligand plus a PPh_3). According to 2D and VT NMR spectroscopy, the solution structures of the two complexes are equivalent to the solid-state ones. For complex $[PPh_3Cu(Br^{Mes}pz^{o-Py})]$, there is an equilibrium involving two different $Br^{Mes}pz^{o-Py}$ ligand conformations, κ^3-S_2H and κ^3-S_2N donor sets, as determined from VT-NMR and DFT calculations. The isomer with a [Cu···H−B] interaction (κ^3-S_2H) is more stable than the one with a pyrazole nitrogen coordination (κ^3-S_2N) of 8.3 kJ/mol (DFT). Furthermore, the hypothesis that the fluxional behavior may be the result of the PPh_3 dissociation has been discredited by NMR titration using a large excess of PPh_3. The ligand conformation of the more stable species was already reported in the parent compound $[Cu(Br^{Mes}pz^{o-Py})]_2$.[1] The B−H involvement into the metal coordination is not a surprising feature, because for analogous boron-centered tripodal ligands, several examples are known to exist in which the Tm and hybrid $pzBm^{Me}$ ligands act in the κ^3-S_2H mode employing the B−H group as an additional binding site.[28]

The only compound of the type [PyCu(L)] for which the formation constant could be determined by NMR was $[PyCu(Tr^{Mes,Me})]$ (slow-exchange condition in the 220−340 K range). Performing Py titration at different temperatures (260−305 K) allowed for the determination of the thermodynamic parameters, suggesting that the Cu−N(Py) interaction is stronger than the Cu···H−B one, making the assumption that an equal number of sulfur atoms are coordinated to copper in the dinuclear complex and in the Py adduct.

The Tu titrations exhibit fast-exchange features above 290 K and are in the slow-exchange regime below this temperature, but unfortunately the determination of ΔH^0 and ΔS^0 was not possible because of the minimal K_f dependence on the temperature. This was related to the equivalence of the copper coordination in the parent $[Cu(Tr^{Mes,Me})]_2$ dimer and in the $[TuCu(Tr^{Mes,Me})]$ derivative that involves three C=S groups and a Cu···H−B interaction, as shown by the X-ray structure analysis.

Acknowledgment. This work was supported by the Ministero dell'Istruzione, dell'Università e Ricerca (Rome, Italy).

Supporting Information Available: X-ray crystallographic data for **1a**, **2a**, and **4** (CIF format). CCDC 292102−292104 contain the supplementary crystallographic data for this paper (www.ccdc.cam.ac.uk/conts/retrieving.html). Stacking plots of the ^{1}H NMR titrations with PPh_3, Tu, and Py; variable temperature ^{1}H NMR spectra of **1**−**2**; and 2D NMR spectra for **1**−**3**. This material is available free of charge via the Internet at http://pubs.acs.org.

IC052129L

(28) (a) Alvarez, H. M.; Tanski, T. M.; Rabinovich, D. *Polyhedron* **2004**, *23*, 395−403. (b) Foreman, M. R. St.-J.; Hill, A. F.; Owen, G. R.; White, A. J. P.; Williams, D. J. *Organometallics* **2003**, *22*, 4446−4450. (c) Kimblin, C.; Churchill, D. G.; Bridgewater, B. M.; Girard, J. N.; Quarless, D. A.; Parkin, G. *Polyhedron* **2001**, *20*, 1891−1896. (d) $PzBm^{Me}$ = bis(mercaptoimidazolyl)(pyrazolyl)hydroborato: Kimblin, C.; Bridgewater, B. M.; Churchill, D. G.; Hascall, T.; Parkin, G. *Inorg. Chem.* **2000**, *39*, 4240−4243.